IJRCS

International Journal of Robotics and Control Systems
Vol. 6, No. 1, 2026, pp. 342-359
ISSN 2775-2658
http://pubs2.ascee.org/index.php/ijrcs

ASCEE

Adaptive Fuzzy Type-3 Fractional-Order Sliding Mode Controller Without Reaching Phase for Underactuated Mechanical Systems

Ali Nasser-Eddine Bendenidina [a,1], Kamel Guesmi [b,2], Aissa Rebai [c,3], Allaeddine Yahia Damani [d,4], Bachir Nail [e,5], Imad Eddine Tibermacine [f,6,*], Alfian Ma'arif [g,7]

[a] Laboratory of Applied Automation and Industrial Diagnostics, Djelfa University, Djelfa, Algeria
[b] Department of Electrical Engineering, Djelfa University, Djelfa, Algeria
[c] Department of Control and Electromechanics, Ghardaia University, Ghardaia, Algeria
[d] Laboratory of Signal and Image Processing, Saad Dahlab University, Blida, Algeria
[e] Renewable Energy Systems Applications Laboratory (LASER), Faculty of Sciences and Technology, Ziane Achour University, Djelfa, Algeria
[f] Department of Computer, Automation and Management Engineering, Sapienza University of Rome, Via Ariosto, 25, 00185 Roma (RM), Rome, Italy
[g] Department of Electrical Engineering, Universitas Ahmad Dahlan, Yogyakarta, Indonesia
[1] a.bendenidina@univ-djelfa.dz; [2] guesmika@univ-djelfa.dz; [3] rebai.aissa@univ-ghardaia.edu.dz;
[4] damaniallaeddine@univ-blida.dz; [5] b.nail@univ-djelfa.dz; [6] tibermacine@diag.uniroma1.it;
[7] alfian.maarif@te.uad.ac.id
[*] Corresponding Author

ARTICLE INFO

Article History
Received September 25, 2025
Revised November 18, 2025
Accepted January 29, 2026

Keywords
Underactuated Mechanical System UMS;
Fractional-Order;
Sliding Mode Control;
Adaptive Fuzzy Type-3

ABSTRACT

This paper presents a adaptive hybrid control strategy for underactuated mechanical systems (UMS). The proposed controller integrates fractional calculus, sliding mode control (SMC), and type-3 fuzzy logic control within a unified framework. A new time-varying switching surface is designed such that the sliding plane passes through the position defined by the system's initial error conditions, thereby eliminating the reaching phase and reducing chattering. The fractional-order operator in the SMC acts as a tunable gain, allowing precise controller adjustment to optimize performance and improve the convergence rate. Moreover, an adaptive Type-3 fuzzy logic system is employed to approximate unknown uncertainties and external disturbances. The stability of the controller is established using Lyapunov theory. Finally, an underactuated crane system is used to validate the proposed approach. Simulation results demonstrate accurate trajectory tracking, effective disturbance rejection, fast convergence (2.98 s), and low tracking error (MSE = 0.00073), confirming the robust performance of the proposed method despite system underactuation.

1. Introduction

In many advanced mechanical and robotic applications, systems are often designed with fewer actuators than degrees of freedom, resulting in what are known as underactuated systems [1]–[3]. This design choice is often motivated by the need to reduce the system weight, cost, complexity, and energy consumption, factors that are critical in aerospace applications [4]–[6], mobile robotics [7]–

[10], and flexible manufacturing [11]–[13]. However, the absence of direct control authority over all degrees of freedom introduces significant challenges in the control design. Unlike fully actuated systems, underactuated ones cannot independently command each state variable, leading to complex nonlinear dynamics and under-constrained control problems.

In recent years, considerable attention has been devoted to tackle these challenges. Among these, predictive control [14]–[16], backstepping technique [17], [18], adaptive control [19]–[23], artificial neural network [24], [25], fuzzy control [26]–[29]. These approaches have demonstrated promising results in trajectory tracking and disturbance rejection. On the other hand, passivity-based [30], [31] and optimal control methods [32], [33] have been employed to address requirements such as energy-efficiency, and stabilization objectives. Sliding Mode Control (SMC), known for its robustness against uncertainties, has been enhanced through hybrid approaches combining adaptive laws, fractional-order calculus, and fuzzy logic to improve convergence, reduce chattering, and handle unknown disturbances.

Recent studies have focused on combining fuzzy logic with adaptive SMC for underactuated systems. For instance, In [34], an adaptive fuzzy SMC was developed to compensate for time-varying sensor faults in underactuated systems, the paper [35] introduces a novel Adaptive Fuzzy SMC technique for Multiple-Input Multiple-Output fractional-order nonlinear systems. Adaptive SMC combined with super-twisting or nonsingular terminal SMC was applied to quadrotor UAVs in [36], [37], showing improved robustness and precision. A new adaptive fuzzy framework for nonlinear underactuated systems with unknown input gain functions was developed in [38].

Type-3 fuzzy logic systems, which extend traditional fuzzy frameworks by incorporating multilevel membership functions to capture deeper uncertainty, have also been explored. For instance, [39] presented a Type-3 FLC for vehicles with fractional-order tuning and a predictive scheme to improve lateral displacement accuracy. A fractional-order dynamic model with a non-singleton interval Type-3 fuzzy system for uncertainty estimation was proposed in [40]. Path-following for mobile robots using Type-3 FLC was studied in [41], while [42] developed a Type-3 fuzzy-based control strategy for robotic manipulator trajectory tracking. Observer-based Type-3 fuzzy SMC strategies were presented in [43] to estimate unknown nonlinear functions online through the design of a novel interval Type-3 FLC.

Hybrid SMC approaches and fractional-order sliding surfaces, which employ non-integer derivatives to enhance system responsiveness and control flexibility, have also been investigated. In [44], fractional derivatives were integrated into a two-level sliding surface ensuring finite-time convergence. Event-triggered backstepping combined with fractional-order SMC was proposed in [45] to enhance attitude and position tracking while estimating unknown disturbances.

Despite these advances, several critical challenges remain unaddressed in the literature. First, most fuzzy–SMC schemes for UMS rely on Type-1 or Type-2 fuzzy logic, only very few studies explore Type-3 fuzzy systems in UMS, and most of those are restricted to robotic, not underactuated. Second, although fractional-order SMC has been investigated, existing methods typically require a reaching phase, leaving the system temporarily exposed to disturbances before convergence, which degrades robustness in practical UMS applications. Third, many hybrid approaches demand prior knowledge of uncertainty.

This paper fills that gap by proposing an adaptive fuzzy type-3 fractional-order sliding mode controller without reaching phase to address the complex dynamics of underactuated mechanical systems. The controller is structured around three key components:

- A novel time-varying switching surface is introduced such that, at the initial moment, the plane intersects the point determined by the system's initial error conditions. This design removes the reaching phase, thereby enhancing system robustness and effectively suppressing chattering.
- The fractional-order, acting as a tunable gain in the sliding mode controller, enables rapid re-

sponse, enhancing convergence speed, and improving overall tracking performance.
- A type-3 fuzzy logic system captures deep levels of uncertainty and disturbance effects through its multi-layered membership structure, which approximates unknown disturbances and manages high levels of uncertainty.

Simulation results conducted on an underactuated crane system, demonstrates superior performance compared with type-1 fuzzy logic sliding mode control SMC–FT1 and type-2 fuzzy SMC–FT2 methods, achieving consistently lower tracking errors. Specifically, it yields an ISE of 0.0364, whereas SMC–FT1 and SMC–FT2 attain 0.0424 and 0.0423, respectively, highlighting enhanced robustness against uncertainties while maintaining precise trajectory tracking. In addition, the controller achieves faster convergence, with times of 0.55s, compared with 1.82s for SMS–FLC-1, and 1.84s for SMS–FLC-2.

The structure of this paper is as follows: Section 2 introduces the dynamic modelling of UMS. Section 3 presents the design of the proposed adaptive fuzzy fractional-order sliding mode control strategy. In Section 4, a comprehensive stability analysis based on Lyapunov theory. Section 5 provides simulation results that validate the effectiveness and performance of the proposed approach. Finally, Section 6 provides conclusions and some directions for future research.

2. UMS Modelling

This study considers an n-degree underactuated mechanical system as a case study. The system's dynamic model is derived by formulating the Lagrangian, expressed as: $l = E_k + E_v$, where E_k is the kinetic energy and E_v represents the potential energy of the system. The Euler–Lagrange equation is then applied to obtain the equations of motion as:

$$\frac{d}{dt}(\frac{\partial l}{\partial q}) - \frac{\partial l}{\partial q} = B(q)u \tag{1}$$

Where u is the control force, $q \in Q$ the configuration vector and $B(q) = (b_i(q), ..., b_m(q)) \in R^{n*m}$ the matrix of external forces. The dynamics of underactuated systems are commonly derived using the Lagrangian or Euler–Lagrange approaches. Accordingly, by applying the Euler–Lagrange formulation, the Lagrangian is formulated as:

$$L(q, \dot{q}) = K - V = \frac{1}{2}\dot{q}^T A(q)\dot{q} - V(q) \tag{2}$$

In vector form, the dynamic equation of UMS can be written as [46] :

$$A\ddot{q} + C(q, \dot{q})\dot{q} + G(q) = B(q)u + d(t) \tag{3}$$

Where $A(q, \dot{q} \in R^{n*n})$ is the inertia matrix and $C(q, \dot{q}) \in R^{n*n}$ Coriolis and centrifugal terms, $G(q) \in R^{n*1}$ is the gravitational force, and $d(t) \in R^m$ denotes the uncertainty term that encompass unknown external disturbances.

The configuration vector is divided into $q = [q_u, q_a]^T$, where $q_u \in R^{n-m}$ denotes the unactuated coordinates, and $q_a \in R^m$ represents the actuated coordinates. Based on this partitioning, the system dynamics are formulated as:

$$\begin{bmatrix} A_u \\ A_a \end{bmatrix} \begin{bmatrix} \ddot{q}_u \\ \ddot{q}_a \end{bmatrix} + \begin{bmatrix} C_u(q, \dot{q}) \\ C_a(q, \dot{q}) \end{bmatrix} \begin{bmatrix} \dot{q}_u \\ \dot{q}_a \end{bmatrix} + \begin{bmatrix} G_u(q) \\ G_a(q) \end{bmatrix} = \begin{bmatrix} 0 \\ u \end{bmatrix} \tag{4}$$

Let the state vector be $x = [x_{2k-1}, x_{2k}] = q = [q_{2k-1}, \dot{q}_{2k-1}]$ the system in (4) can be represented in state-space notation as [47]:

$$\begin{pmatrix} \dot{x}_{2k-1} \\ \dot{x}_{2k} \end{pmatrix} = \begin{pmatrix} x_{2k} \\ h_k(x) \end{pmatrix} + \begin{pmatrix} 0 \\ j_k(x) \end{pmatrix} U + \begin{pmatrix} 0 \\ d(x)_k \end{pmatrix} \tag{5}$$

This model embodies the key dynamic characteristics of underactuated systems, preserving their intrinsic nonlinearity, coupling, and disturbance sensitivity. As such, it serves as an effective benchmark for developing and testing advanced control methods, with outcomes that can be generalized to a wide array of practical UMS. To maintain stability, the switching gain k in conventional SMC must be chosen such that k exceeds $d(x)_k$ in accordance with Assumption 1.

Definition 2.1. A system is qualified as underactuated if the rank of its control input space, m, is strictly less than its degrees of freedom n, i.e., $m < n$.

Assumption 1. The uncertain terms of the system are considered as: $|d_k(x)| \leq \rho_k$, where ρ_k are known positive constants.

3. Design of the Adaptive Fuzzy Type-3 Fractional SMC

The control challenge of underactuated plants stems from the fact that $m < n$. Indeed, the number of control inputs m is fewer than the number of system states n, which implies that not all states can be directly controlled. This issue requires a control strategy that can regulate internal dynamics while driving the outputs toward the desired behaviour.

Based on this fact, the control objective of this study is to design a robust control strategy capable of stabilizing the underactuated system while ensuring accurate tracking performance in the presence of model uncertainties and external disturbances.

As mentioned above, the control objective is to determine a robust Adaptive fuzzy type-3 fractional sliding mode control law $U(x)$ for the nonlinear system given by (5) such that the vector y can follow a given desired reference signal vector yd, in the presence of external disturbances.

3.1. Fractional FTSMC

The linear dynamics are imposed by the selected sliding surface [48] :

$$s = (\frac{d}{dt} + c)^{n-1}e = c_1 e + c_2 \dot{e} + ... + c_{n-1}e^{n-2} + e^{n-1} \tag{6}$$

$$s = e^{n-1} + \sum_{i=0}^{n-2} c_{i+1}e^i \tag{7}$$

Where $e = y_d - y$ is the tracking error, and c_i are positive constants. Aiming to eliminate the reaching phase and achieve finite-time convergence, robust performance, and precise control of the underactuated system, we present a fractional-order integral sliding mode (FO-ISMC) surface that is designed using the framework of fractional calculus as:

$$S = e^{n-1} + \sum_{i=0}^{n-2} c_{i+1}e^i + aD^{-\beta}e + \Psi(e^{n-1}(0) + \sum_{i=0}^{n-2} c_{i+1}e^i(0) + aD^{-\beta}e(0)) \tag{8}$$

We propose the following form of Ψ :

$$\Psi = -exp(t/T)^{\kappa} \tag{9}$$

Where T,a and κ are positive constants, chosen via simulation studies to strike a balance between fast convergence and smooth control behavior. We set: $s_0 = e^{n-1}(0) + \sum_{i=0}^{n-2} c_{i+1}e^i(0) + aD^{-\beta}e(0)$ where s_0 is the initial sliding surface value, the term Ψs_0 ensuring that the sliding manifold passes through the position defined by the system's initial error. The time-varying surface eliminates the reaching phase, and the presence of term Ψ enables the system to react quickly to rapid changes, thereby improving the convergence rate enhancing robustness and reducing chattering, while the

fractional-order improv performance and convergence, and $D^{\alpha_i}e^i$ the fractional derivatives of e^i with respect to β-order. The Riemann–Liouville fractional integral and derivative of order β for a function f, with respect to t are [49]:

$$I^{\beta}f(t) = \frac{1}{\Gamma(\beta)}\int_0^t (t-\tau)^{\beta-1}f(\tau)\,d\tau \tag{10}$$

$$D_t^{\beta}f(t) = \frac{d^n}{dt^n}\left[\frac{1}{\Gamma(n-\beta)}\int_0^t (t-\tau)^{n-\beta-1}f(\tau)\,d\tau\right] \tag{11}$$

Here, D and I represent the fractional derivative and fractional integral operators, respectively, and n is an integer number, $\Gamma(.)$ is Euler's Gamma function given by:

$$\Gamma(z) = \int_0^{\infty} t^{z-1}e^{-t}\,dt \tag{12}$$

This form combines the instantaneous rate of change e^{n-1} with the history-dependent behaviour $D^{\alpha_i}e^i$, giving the controller both fast response and long-term correction capability. By differentiating the sliding surfaces in (8) with respect to time, we obtain:

$$\dot{S} = e^n + \sum_{i=0}^{n-1} c_{i+1}e^i + aD^{1-\beta}e = x^n - x_r^n + \sum_{i=0}^{n-1} c_{i+1}e^i + aD^{1-\beta}e + \dot{\Psi}s_0 \tag{13}$$

By substituting the dynamics:

$$\dot{s} = h(x) + j(x)u + d - \ddot{x}_r + \sum_{i=0}^{n-1} c_{i+1}e^i + aD^{1-\beta}e + \dot{\Psi}s_0 \tag{14}$$

Then the control law is:

$$u = \frac{-1}{j(x)}(h(x) + d(t) - \ddot{x}_r + \sum_{i=0}^{n-1} c_{i+1}e^i + aD^{1-\beta}e + u_{sw} + \dot{\Psi}s_0) \tag{15}$$

We take the switching control as $u_{sw} = k_1 s + k_2 tanh(s)$ with the hyperbolic tangent function defined as $tanh(s) = \frac{e^s - e^{-s}}{e^s + e^{-s}}$.

Since the disturbance is unknown, our next goal is to estimate $d_k(x)$ using a type-3 fuzzy estimator: $\hat{d}_k(x) \approx d_k(x), k = 1...n$. Type-3 fuzzy systems extend the capabilities of Type-1 and Type-2 approaches by introducing an additional layer of membership functions. This allows for more accurate representation of complex uncertainties, which is crucial in UMS due to their strongly nonlinear behavior caused by underactuation and coupled states.

3.2. Type-3 Fuzzy Systems

Recent advances in computational intelligence have driven the evolution of fuzzy logic systems beyond conventional Type-1 [50]–[52] and interval-based Type-2 architectures [53]–[55]. Type-3 fuzzy systems [56]–[58] emerge as a generalized framework characterized by layered uncertainty representation through higher-order membership functions and dynamic footprint-of-uncertainty bounds. Unlike their predecessors, these systems employ secondary membership grades to model complex uncertainty propagation mechanisms, particularly in systems with non-stationary noise distributions or deep epistemic uncertainties. Key challenges include computational complexity management and stability analysis under time-varying uncertainty, which represents an active research area in modern fuzzy control theory.

In this section, the T3FLS will be used in equation (5) where the input variables are x_i. The fuzzy sets of all inputs are denoted by $\Lambda_i^k, \overline{\Omega}_j$, the i^{th} input variable of T3FLS is denoted by χ_i. The general scheme is given by Fig. 1 and the memberships are expressed as [39]:

$$\overline{\zeta}_{\Lambda_i^k,\overline{\Omega}_j}(\chi_i(t)) = \exp\left(-\frac{(\chi_i(t) - m_{\Lambda_i^k,\overline{\Omega}_j})}{\overline{\sigma}^2_{\Lambda_i^k,\overline{\Omega}_j}}\right). \tag{16}$$

$$\overline{\zeta}_{\Lambda_i^k,\underline{\Omega}_j}(x_i(t)) = \exp\left(-\frac{(\chi_i(t) - m_{\Lambda_i^k,\underline{\Omega}_j})}{\overline{\sigma}^2_{\Lambda_i^k,\underline{\Omega}_j}}\right). \tag{17}$$

$$\underline{\zeta}_{\Lambda_i^k,\overline{\Omega}_j}(\chi_i(t)) = \exp\left(-\frac{(\chi_i(t) - m_{\Lambda_i^k,\overline{\Omega}_j})}{\underline{\sigma}^2_{\Lambda_i^k,\overline{\Omega}_j}}\right). \tag{18}$$

$$\underline{\zeta}_{\Lambda_i^k,\underline{\Omega}_j}(\chi_i(t)) = \exp\left(-\frac{(\chi_i(t) - m_{\Lambda_i^k,\underline{\Omega}_j})}{\underline{\sigma}^2_{\Lambda_i^k,\underline{\Omega}_j}}\right). \tag{19}$$

Where $m_{\Lambda_i^k}$ and $\overline{\sigma}_{\Lambda_i^{hi}}$, $\underline{\sigma}_{\Lambda_i^{hi}}$ are centre and upper/lower standard divisions.

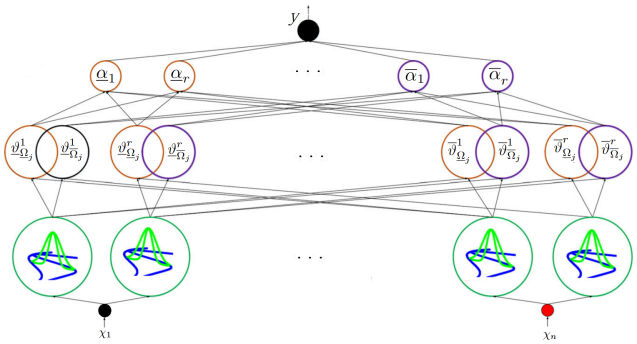

Fig. 1. Diagram of T3-FLS

For rules firing, we have:

$$\overline{\vartheta}^l_{\overline{\Omega}_j} = \prod_{i=1}^{n} \overline{\zeta}_{\Lambda_i^{ki},\overline{\Omega}_j} \tag{20}$$

$$\overline{\vartheta}^l_{\underline{\Omega}_j} = \prod_{i=1}^{n} \overline{\zeta}_{\Lambda_i^{ki},\underline{\Omega}_j} \tag{21}$$

$$\underline{\vartheta}^l_{\overline{\Omega}_j} = \prod_{i=1}^{n} \underline{\zeta}_{\Lambda_i^{ki},\overline{\Omega}_j} \tag{22}$$

$$\underline{\vartheta}^l_{\underline{\Omega}_j} = \prod_{i=1}^{n} \underline{\zeta}_{\Lambda_i^{ki},\underline{\Omega}_j} \tag{23}$$

The form of l^{th} rule is given as:
If x_1 is Λ^{k1}_{1,A_j} and x_2 is Λ^{k2}_{2,A_j} ...and x_n is Λ^{kn}_{n,A_j} **Then** $y_l \in [\underline{\alpha}_{l,j}, \overline{\alpha}_{l,j}]$.
Where $\underline{\alpha}_{l,j}, \overline{\alpha}_{l,j}$ denotes the upper/lower bounds of l^{th} type-3 interval FS, and y_l denotes the output

of the fuzzy system at the l^{th} rule.
The output of the T3FS can be written as:

$$y = \frac{\sum_{j=1}^{k}}{\sum_{j=1}^{k} \overline{\Omega}_j} \left(\frac{\sum_{l=1}^{r} \overline{\Omega}_j (\overline{\vartheta}_{\overline{\Omega}_j}^{l} + \underline{\vartheta}_{\overline{\Omega}_j}^{l}) \overline{\alpha}_{l,j}/2}{\sum_{l=1}^{r} (\overline{\vartheta}_{\overline{\Omega}_j}^{l} + \underline{\vartheta}_{\overline{\Omega}_j}^{l})} + \underline{\Omega}_j \frac{\sum_{l=1}^{r} (\overline{\vartheta}_{\underline{\Omega}_j}^{l} + \underline{\vartheta}_{\underline{\Omega}_j}^{l}) \underline{\alpha}_{l,j}/2}{\sum_{l=1}^{r} (\overline{\vartheta}_{\underline{\Omega}_j}^{l} + \underline{\vartheta}_{\underline{\Omega}_j}^{l})} \right) \tag{24}$$

The output can be rewritten as:

$$y = \alpha^T \Phi \tag{25}$$

Where shown in Fig. 2,

$$\begin{aligned} \alpha^T = [&\underline{\alpha}_{1,\underline{\Omega}_1}, ..., \underline{\alpha}_{1,\underline{\Omega}_k}, ..., \underline{\alpha}_{r,\underline{\Omega}_r}, ..., \underline{\alpha}_{r,\underline{\Omega}_r} \\ &\underline{\alpha}_{1,\overline{\Omega}_1}, ..., \underline{\alpha}_{1,\overline{\Omega}_k}, ..., \underline{\alpha}_{r,\overline{\Omega}_r}, ..., \underline{\alpha}_{r,\overline{\Omega}_r} \\ &\overline{\alpha}_{1,\underline{\Omega}_1}, ..., \overline{\alpha}_{1,\underline{\Omega}_k}, ..., \overline{\alpha}_{r,\underline{\Omega}_r}, ..., \overline{\alpha}_{r,\underline{\Omega}_r} \\ &\overline{\alpha}_{1,\overline{\Omega}_1}, ..., \overline{\alpha}_{1,\overline{\Omega}_k}, ..., \overline{\alpha}_{r,\overline{\Omega}_r}, ..., \overline{\alpha}_{r,\overline{\Omega}_r}] \end{aligned} \tag{26}$$

$$\begin{aligned} \Phi^T = \frac{0.5}{\sum_{j=1}^{k} \overline{\Omega}_j} \Bigg(&\frac{\underline{\Omega}_1 (\overline{\vartheta}_{\underline{\Omega}_1}^{1} + \underline{\vartheta}_{\underline{\Omega}_1}^{1})}{\sum_{l=1}^{r} (\overline{\vartheta}_{\underline{\Omega}_j}^{1} + \underline{\vartheta}_{\underline{\Omega}_j}^{1})}, ..., \underline{\Omega}_k \frac{\underline{\Omega}_k (\overline{\vartheta}_{\underline{\Omega}_k}^{1} + \underline{\vartheta}_{\underline{\Omega}_k}^{1})}{\sum_{l=1}^{r} (\overline{\vartheta}_{\underline{\Omega}_1}^{1} + \underline{\vartheta}_{\underline{\Omega}_1}^{1})} \\ &, \frac{\underline{\Omega}_1 (\overline{\vartheta}_{\underline{\Omega}_1}^{r} + \underline{\vartheta}_{\underline{\Omega}_1}^{r})}{\sum_{l=1}^{r} (\overline{\vartheta}_{\underline{\Omega}_j}^{r} + \underline{\vartheta}_{\underline{\Omega}_j}^{r})}, ..., \underline{\Omega}_k \frac{\underline{\Omega}_k (\overline{\vartheta}_{\underline{\Omega}_k}^{r} + \underline{\vartheta}_{\underline{\Omega}_k}^{r})}{\sum_{l=1}^{r} (\overline{\vartheta}_{\underline{\Omega}_1}^{r} + \underline{\vartheta}_{\underline{\Omega}_1}^{r})} \\ &, \frac{\overline{\Omega}_1 (\overline{\vartheta}_{\overline{\Omega}_1}^{1} + \underline{\vartheta}_{\overline{\Omega}_1}^{1})}{\sum_{l=1}^{r} (\overline{\vartheta}_{\overline{\Omega}_j}^{1} + \underline{\vartheta}_{\overline{\Omega}_j}^{1})}, ..., \overline{\Omega}_k \frac{\overline{\Omega}_k (\overline{\vartheta}_{\overline{\Omega}_k}^{1} + \underline{\vartheta}_{\overline{\Omega}_k}^{1})}{\sum_{l=1}^{r} (\overline{\vartheta}_{\overline{\Omega}_1}^{1} + \underline{\vartheta}_{\overline{\Omega}_1}^{1})} \\ &, \frac{\overline{\Omega}_1 (\overline{\vartheta}_{\overline{\Omega}_1}^{r} + \underline{\vartheta}_{\overline{\Omega}_1}^{r})}{\sum_{l=1}^{r} (\overline{\vartheta}_{\overline{\Omega}_j}^{r} + \underline{\vartheta}_{\overline{\Omega}_j}^{r})}, ..., \overline{\Omega}_k \frac{\overline{\Omega}_k (\overline{\vartheta}_{\overline{\Omega}_k}^{r} + \underline{\vartheta}_{\overline{\Omega}_k}^{r})}{\sum_{l=1}^{r} (\overline{\vartheta}_{\overline{\Omega}_1}^{r} + \underline{\vartheta}_{\overline{\Omega}_1}^{r})} \Bigg) \end{aligned} \tag{27}$$

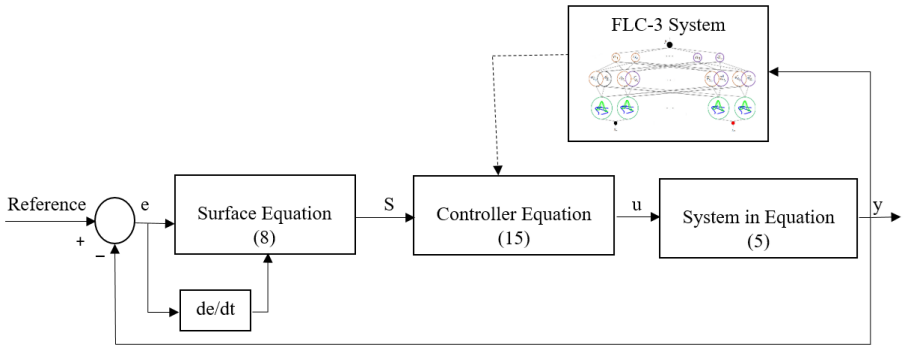

Fig. 2. Block diagram of the proposed approach

4. Stability Analysis

Theorem 1. Using the sliding surface (8), the control law (15) guarantees the asymptotic convergence of the system (5) to the reference trajectory and the tracking error e to zero.

Proof. Let the Lyapunov candidate function:

$$V = \frac{1}{2}s^2 + \frac{1}{2\Gamma}\tilde{\alpha}^T\tilde{\alpha} \tag{28}$$

Here, $\tilde{\alpha} = \alpha^* - \alpha$ is the fuzzy parameter estimation error, and Γ is a positive definite adaptation gain. Its time derivative is:

$$\dot{V} = S\dot{S} + \tilde{\alpha}^T\Gamma^{-1}\dot{\alpha} \tag{29}$$

$$\dot{V} = S[h(x) + j(x)u + d - \ddot{x}_r + \sum_{i=0}^{n-1} c_{i+1}e^i + aD^{1-\beta}e + \dot{\Psi}s_0] + \tilde{\alpha}^T\Gamma^{-1}\dot{\alpha} \tag{30}$$

Adding and subtracting the optimal fuzzy approximation $\hat{d}^*$ yields:

$$\dot{V} = S[h(x) + j(x)u + d - \ddot{x}_r + \sum_{i=0}^{n-1} c_{i+1}e^i + aD^{1-\beta}e\dot{\Psi}s_0 + \hat{d}^* - \hat{d}^*] + \tilde{\alpha}^T\Gamma^{-1}\dot{\tilde{\alpha}} \tag{31}$$

By definition, the fuzzy estimation error can be expressed as:

$$[\hat{d}^* - \hat{d}] = (\alpha^* - \alpha)^T\Phi = \tilde{\alpha}^T\Phi \tag{32}$$

The optimal error is defined as:

$$\epsilon = d - \hat{d}^* \tag{33}$$

Substituting (32) and (33) in (31) leads to:

$$\begin{aligned}\dot{V} &= S[\epsilon + \tilde{\alpha}^T\Phi - K_1S - K_2sgn(S)] + \tilde{\alpha}^T\Gamma^{-1}\dot{\tilde{\alpha}} \\ &= S\epsilon + S\tilde{\alpha}^T\Phi - K_1S^2 - K_2|S| + \tilde{\alpha}^T\Gamma^{-1}\dot{\tilde{\alpha}}\end{aligned} \tag{34}$$

Since $\tilde{\alpha} = \alpha^* - \alpha$, we can obtain $\dot{\tilde{\alpha}} = -\dot{\alpha}$ leading to:

$$\dot{V} = S\epsilon + S\tilde{\alpha}^T\Phi - K_1S^2 - K_2|S| - \tilde{\alpha}^T\Gamma^{-1}\dot{\alpha} \tag{35}$$

Rewriting, we obtain:

$$\dot{V} = -K_1S^2 - K_2|S| + S\epsilon + \tilde{\alpha}^T(S\Phi - \Gamma^{-1}\dot{\alpha}) \tag{36}$$

Hence, the corresponding tuning laws are chosen as:

$$\dot{\alpha} = -\Gamma S\Phi \tag{37}$$

Substituting (37) into (36) yields:

$$\dot{V} = -K_1S^2 - K_2|S| + S\epsilon \tag{38}$$

we have $S\epsilon \leq |S||\epsilon|$ Hence:

$$\dot{V} \leq |S|(|\epsilon| - K_2) - K_1S^2 \tag{39}$$

Equation (39) establishes that the global sliding surface is stable, guaranteeing the overall stability of the closed-loop system when the control gain satisfies $K_2 \leq |\epsilon|$. Under this condition, the tracking error converges to a small neighborhood around zero, thereby demonstrating the robustness and effectiveness of the proposed controller. □

5. Simulation Results

To evaluate the effectiveness and robustness of the proposed controller, the MATLAB platform was used to assess the proposed controller's performance on the crane model shown in Fig. 3, considered as an underactuated system with two degrees of freedom.

The system dynamic equations can be expressed in state-space form, using the state vector $\begin{bmatrix} x_1 & x_2 & x_3 & x_4 \end{bmatrix}^T = \begin{bmatrix} x & \dot{x} & \theta & \dot{\theta} \end{bmatrix}^T$ where the nonlinear functions h_1, j_1, h_2 and j_2 are defined as [59]:

$$\begin{aligned} h_1 &= \frac{(-m_p^2 l^2 g cos(\theta) sin(\theta + m_p l^2 (m_p l \dot{\theta}^2 sin(\theta) - D\dot{x})}{m_p l^2 (m_c + m_p (1 - cos(\theta)^2))} \\ j_1 &= \frac{m_p l^2}{m_p l^2 (m_c + m_p (1 - cos(\theta)^2))} \\ h_2 &= \frac{(m_p + m_c) m_p g l sin(\theta) - m_p l cos(\theta)(m_p l \dot{\theta}^2 sin(\theta) - D\dot{x})}{m_p l^2 (m_c + m_p (1 - cos(\theta)^2))} \\ j_2 &= \frac{m_p l cos(\theta)}{m_p l^2 (m_c + m_p (1 - cos(\theta)^2))} \end{aligned} \tag{40}$$

The crane system's parameters and variables are summarized in the Table 1.

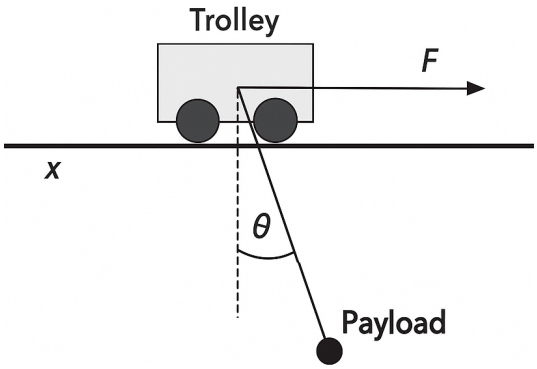

Fig. 3. Crane system

Table 1. Variables and parameters of the crane

Symbols	Description
x	Position of the cart
$\dot{x}$	Velocity of the cart
θ	Angle of the payload
$\dot{\theta}$	Angular velocity of the payload
m_p	Mass of the payload
m_c	Trolley's mass
l	Rope length
g	Gravity acceleration
D	Damping factor

The control objective is to drive the crane to a specified target position while ensuring that the pendulum angle remains at zero. The initial conditions are specified as follows:$x = \begin{bmatrix} 0.8 & 0 & 0.1 & 0 \end{bmatrix}^T$, with the desired trajectory $cos(0.5 * t)$.

The simulation parameters of the crane are $m_p = 6, m_c = 9, l = 2, g = -9.81, D = 0.5$, and parameters of the controller are $k1 = 0.1, k2 = 10, c1 = 0.5, c2 = 5, a = 0.5, \beta = 0.1$, and

$[-m_{\Lambda_i^1}, -m_{\Lambda_i^2}, -m_{\Lambda_i^3}] = [-\pi/5, 0, \pi/5]$, $\overline{\sigma}_{\Lambda_i^k} = 1$ $\underline{\sigma}_{\Lambda_i^k} = 0.5$. We consider four rules and three membership functions, and we chose $D1 = D2 = 0.05 * sin(.05 * t) + .3 * exp(-((t - 1120)^2)/(2 * 50^2))$.

The dynamic behavior of the system under the proposed control law is illustrated in Fig. 4. It can be observed that the controller is able to precisely drive the trolley along the reference trajectory toward the target location while simultaneously reducing the oscillatory motion of the suspended payload. The rapid damping of these oscillations within a relatively short time interval demonstrates not only the accuracy of the positioning task but also the controller's effectiveness in stabilizing the underactuated dynamics. Furthermore, Fig. 5 highlights the controller's capacity to rapidly attenuate payload swing, which is a critical challenge in overhead crane systems.

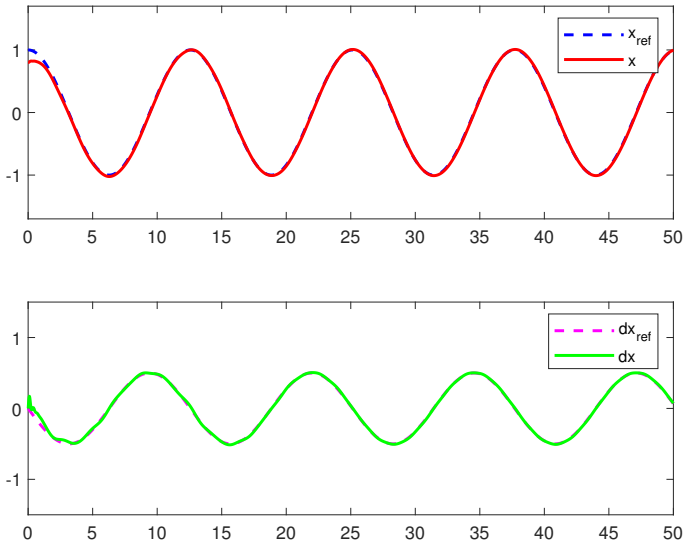

Fig. 4. Performances of x and $\dot{x}$

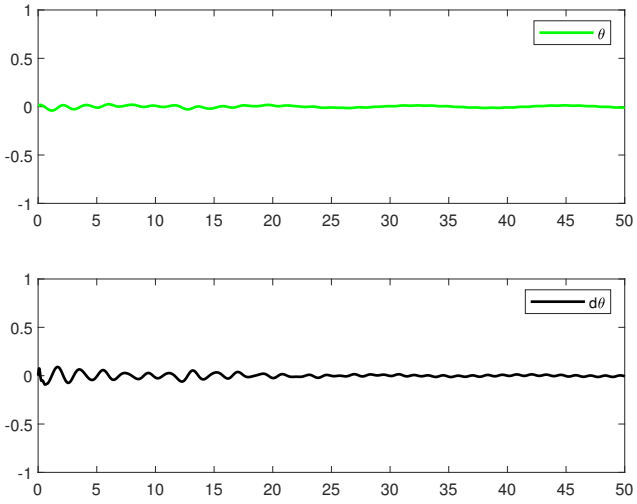

Fig. 5. Performances of θ and $\dot{\theta}$

The results show that oscillations are efficiently suppressed during the motion process, preventing destabilizing effects and ensuring smooth overall system behavior. This effective swing reduction confirms the robustness of the proposed control method in handling underactuated dynamics and enhancing operational safety, particularly in tasks where minimizing residual vibrations is of primary importance. A detailed examination of the tracking errors presented in Fig. 6 provides clear evidence of the efficiency of the proposed control strategy.

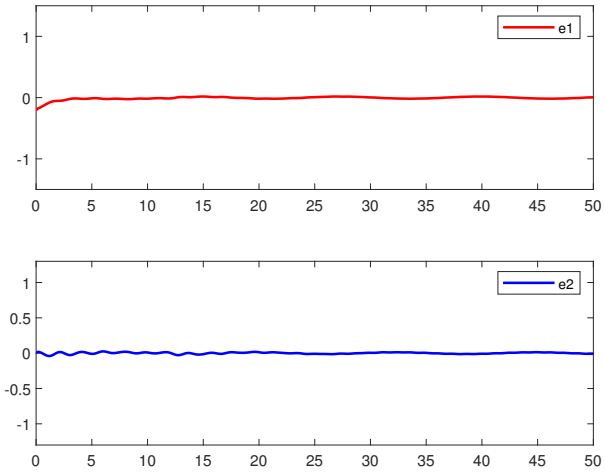

Fig. 6. Tracking errors e_1 and e_2

It can be observed that both error signals converge rapidly toward zero, which highlights the controller's ability to achieve fast transient dynamics. The short convergence time indicates that the control input is capable of compensating for the nonlinearities of the system without inducing significant overshoot or oscillatory behavior. More importantly, the accuracy is preserved even under system uncertainties and external disturbances, which underlines the robustness and reliability of the proposed scheme for practical applications. Fig. 7 illustrates the behaviour of the control signal u and the sliding surface S.

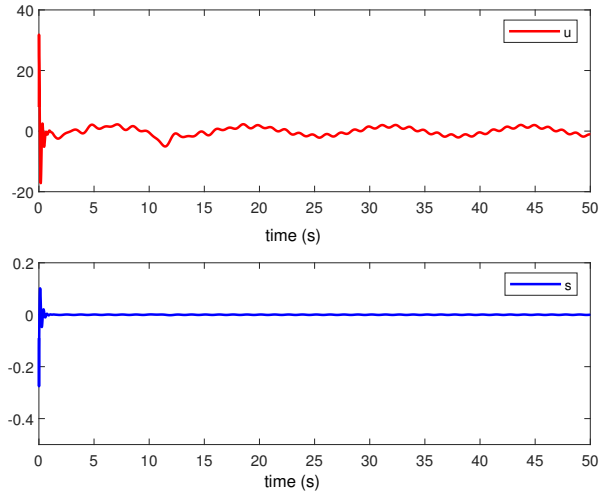

Fig. 7. Control action u and sliding surface S

These results show that the control input remains bounded while effectively driving the system states toward the sliding surface. The surface S converges rapidly to zero, confirming that the sliding mode condition is satisfied and the system operates within the designed control dynamics.

For comparison, the performance of the proposed control strategy is evaluated against the method presented in [60] which employs a sliding mode controller (SMC) enhanced with a fuzzy disturbance observer, and an improved version incorporating a Type-2 Fuzzy Logic Controller, where x flc1, dx flc1,θ flc1,$\dot{\theta}$ flc1,e flc1, and x flc2, dx flc2,θ flc2,$\dot{\theta}$ flc2,e flc2, represent the results from SMC withe FLC type-1 in [60] and FLC type-2 respectivly, and x_P, dxP,θP, $\dot{\theta}P$ and eP correspond to the outcomes of the proposed control method.

Fig. 8, Fig. 9, and Fig. 10 collectively offer a thorough performance assessment of the system states and tracking errors under identical operating conditions. Figure Fig. 8 examines the evolution of x and dx , where the proposed control scheme exhibits quicker settling behavior, and a smaller steady–state deviation when compared with withe the outer. The responses of θ and $\dot{\theta}$ in Fig. 9 further reinforce this trend, showing closer alignment with the desired reference paths. Fig. 10 focuses on the error signals e_1 and e_2 which decay more rapidly and maintain consistently lower magnitudes under the proposed controller. The enlarged sections within these figures clearly highlight that the introduced method achieves more precise trajectory tracking and overall enhanced performance relative to previously reported techniques.

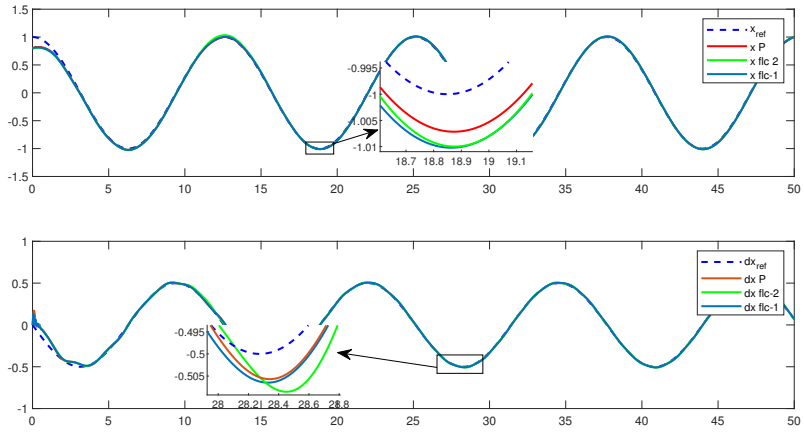

Fig. 8. Comparison in terms of x and $\dot{x}$

Table 2 presents a detailed comparison of trajectory tracking performance. The tracking error indices, including RMSE, ISE, IAE, MSE, ITAE, and variance, were calculated according to the equations in Table 3. These results provide a quantitative assessment of controller accuracy and demonstrate the superior performance of the proposed method compared to existing SMS-FLC variants.

Across all evaluated metrics, the proposed controller consistently achieves lower errors. as an illustration, it achieves an ISE of 0.0364, whereas the SMC–FT1 approach in [60] yields 0.0424 and the SMC–FT2 method attains 0.0423.

Resulting in more precise trajectory tracking. The convergence times for e_1 and e_2 are 3.15 s and 0.55 s, respectively, under the proposed controller, compared with 10.45 s and 1.82 s for SMS-FLC-1 in [60], and 10.50 s and 1.84 s for SMS-FLC-2. The most notable improvements are observed in e_1, indicating faster convergence. Overall, these findings confirm that the proposed controller enhances robustness against uncertainties and external disturbances while maintaining high tracking accuracy.

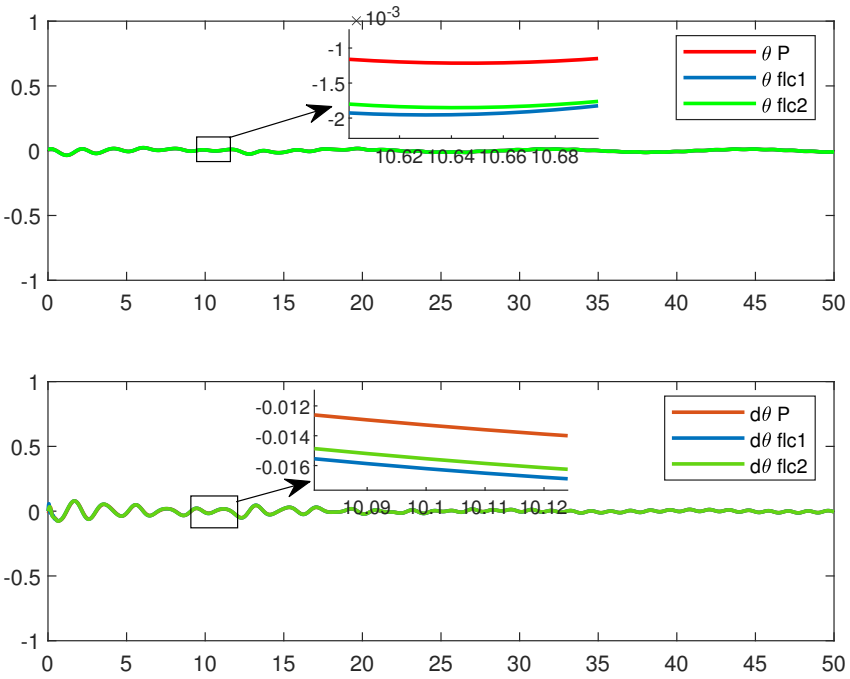

Fig. 9. Comparison in terms of $\dot{\theta}$ and θ

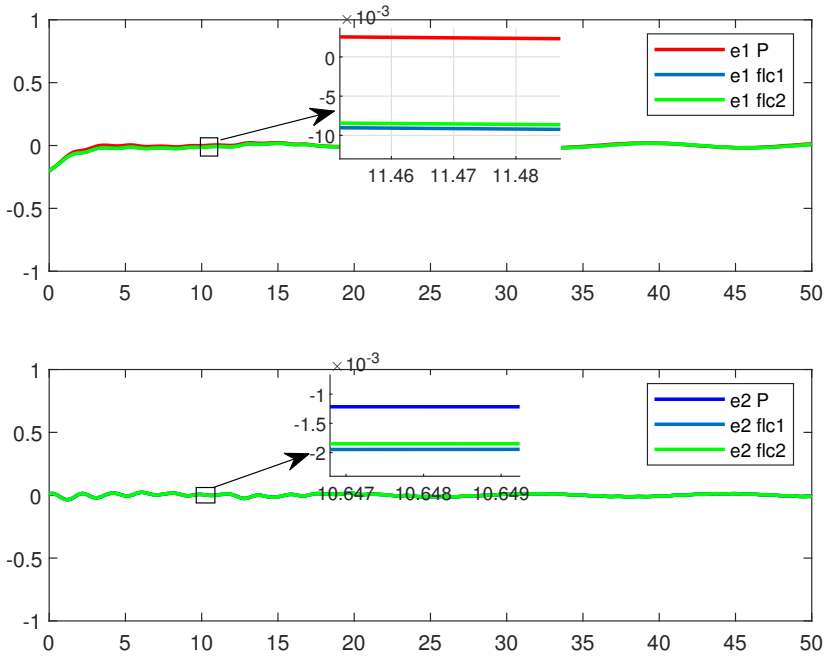

Fig. 10. Comparison in terms of e_1 and $e2$

Furthermore, the proposed controller achieves the desired performance while consuming (110.50) of control energy, which is lower than SMS-FLC-1 (124.62) and comparable to SMS-FLC-2 (109.01).

Table 2. Quantitative comparison of trajectory tracking performance for e_1 and e_2 under the proposed controller and SMS-FLC1, SMS-FLC1 controller

Controller	Error	RMSE	ISE	IAE	MSE	ITAE	TV
Proposed Controller	e_1	0.0270	0.0364	0.7213	0.00073	13.7967	0.000722
	e_2	0.0099	0.0042	0.4115	0.00009	9.3465	0.000098
SMS-FLC2	e_1	0.0291	0.0423	0.8580	0.00085	14.5388	0.000767
	e_2	0.0100	0.0049	0.4135	0.00010	9.3473	0.000099
SMS-FLC1 [60]	e_1	0.0292	0.0424	0.8601	0.00086	14.5765	0.000769
	e_2	0.0102	0.0050	0.4141	0.00011	9.3611	0.00010

Table 3. Performance indices used for tracking evaluation

Index	Equation	Description
MSE	$\text{MSE} = \frac{1}{T}\int_0^T e^2(t)\,dt$	Mean Squared Error; average of squared tracking error over simulation time.
RMSE	$\text{RMSE} = \sqrt{\frac{1}{T}\int_0^T e^2(t)\,dt}$	Root Mean Squared Error; provides typical magnitude of tracking error.
ISE	$\text{ISE} = \int_0^T e^2(t)\,dt$	Integral of Squared Error; penalizes large errors heavily.
IAE	$\text{IAE} = \int_0^T \lvert e(t)\rvert\,dt$	Integral of Absolute Error; accumulates absolute error over time.
ITAE	$\text{ITAE} = \int_0^T t\,\lvert e(t)\rvert\,dt$	Integral of Time-weighted Absolute Error; emphasizes long-lasting errors and settling behavior.
TV	$\text{TV} = \frac{1}{T}\int_0^T (e(t)-\bar{e})^2\,dt$	Tracking Variance, measures variability of the tracking error around its mean; indicates smoothness and stability.
The control energy	$E_u = \int_0^T u^2(t)\,dt$	Measures the total actuator effort required by the controller over the simulation duration

Note: $e(t)$ represents the tracking error, and $\bar{e}$ denotes the mean value of $e(t)$ over the interval $[0, T]$. Δt is the sampling period. This text will automatically wrap to multiple lines inside the table cell if it exceeds the width.

These results confirm that the proposed method not only enhances robustness against uncertainties and external disturbances but also provides efficient control with reduced actuator effort. However, a noted limitation is that the energy consumption is still approximately on par with other controllers. This could be mitigated by implementing an event-triggered control strategy, updating the control signal only when necessary, which would reduce computational demands and communication load.

6. Conclusion

In this study, presents a adaptive hybrid adaptive fuzzy Type-3 fractional-order sliding mode controller strategy for underactuated mechanical systems (UMS). The proposed controller utilized a novel time-varying switching surface to eliminate the reaching phase achieves higher robustness and mitigates the chattering effect, while the Fractional-order implementation yielded faster convergence and smoother transient behavior. To estimate unknown disturbances, an adaptive Type-3 fuzzy inference system is utilized.

The results indicate that the developed control strategy exhibits enhanced robustness and high tracking accuracy in comparison with traditional schemes, thereby providing a solid basis for further developments in the control of complex underactuated mechanical systems. Moreover, the proposed methodology can be generalized to higher-order UMS, where the increasing complexity of system dynamics demands more effective integration of fractional-order control and adaptive fuzzy mecha-

nisms. The limitation of energy consumption can be mitigated through the use of an event-triggered control strategy.

As future work, the integration of a predictive control scheme will be considered to improve decision-making over a finite horizon and enhance the controller's performance in dynamic environments. Additionally, implementing an event-triggered control strategy can reduce computation and communication by updating the control signal only when necessary, thereby improving efficiency, enhancing responsiveness, and reducing energy consumption.

Author Contribution: All authors contributed equally to the main contributor to this paper. All authors read and approved the final paper.

Funding: This research received no external funding

Acknowledgment: The author expresses sincere gratitude to the colleagues and peers for their insightful discussions and encouragement, which greatly contributed to the completion of this thesis.

Conflicts of Interest: The authors declare that they have no conflict of interest.

References

[1] M. Zhai, N. Sun, T. Yang, and Y. Fang, "Underactuated mechanical systems with both actuator and actuated/unactuated state constraints: A predictive control-based approach," *IEEE/ASME Transactions on mechatronics*, vol. 28, no. 3, pp. 1359–1371, 2022, https://doi.org/10.1109/TMECH.2022.3230244.

[2] S. Jadlovska, A. Jadlovska, M. Uhlar, and J. Pitel, "Modeling and optimal control of underactuated mechanical systems," in *AIP Conference Proceedings*, vol. 3094, 2024, https://doi.org/10.1063/5.0212921.

[3] E. Franco and K. Chen, "Integral ida-pbc for underactuated mechanical systems with unmeasured actuator dynamics and time-varying matched disturbances," *European Journal of Control*, vol. 85, p. 101256, 2025, https://doi.org/10.1016/j.ejcon.2025.101256.

[4] L. Jin and Y. Li, "Model predictive control-based attitude control of under-actuated spacecraft using solar radiation pressure," *Aerospace*, vol. 9, no. 9, p. 498, 2022, https://doi.org/10.3390/aerospace9090498.

[5] C. Yue, M. Lu, X. Ju, X. Chen, and Q. Shen, "Hierarchical attitude stabilization controller design and analysis for underactuated spacecraft on so (3)," *Aerospace Science and Technology*, vol. 155, p. 109535, 2024, https://doi.org/10.1016/j.ast.2024.109535.

[6] S. Chernyshev, K. Sypalo, and S. Bazhenov, "Intelligent control algorithms to ensure the flight safety of aerospace vehicles," *Acta Astronautica*, vol. 226, pp. 782–790, 2025, https://doi.org/10.1016/j.actaastro.2024.10.073.

[7] P. Liu and S. Tong, "A finite-time fuzzy adaptive output-feedback fault-tolerant control for underactuated wheeled mobile robots systems," *Journal of Automation and Intelligence*, vol. 3, no. 2, pp. 111–118, 2024, https://doi.org/10.1016/j.jai.2024.02.005.

[8] A. Y. Damani, Z. A. Benselama, and R. Hedjar, "Formation control of nonholonomic wheeled mobile robots via fuzzy fractional-order integral sliding mode control," *International Journal of Dynamics and Control*, vol. 11, no. 5, pp. 2273–2284, 2023, https://doi.org/10.1007/s40435-022-01109-x.

[9] P. Liu and S. Tong, "Fuzzy adaptive fault-tolerant control for underactuated wheeled mobile robot with prescribed performance," *International Journal of Control, Automation and Systems*, vol. 22, no. 6, pp. 1998–2006, 2024, https://doi.org/10.1007/s12555-023-0454-z.

[10] Z. Zhao, X. Li, S. Liu, M. Zhou and X. Yang, "Multi-Mobile-Robot Transport and Production Integrated System Optimization," in *IEEE Transactions on Automation Science and Engineering*, vol. 22, pp. 7480-7491, 2025, https://doi.org/10.1109/TASE.2024.3421889.

[11] L. Zhao, F. Guo, F. Yang, C. Li, Y. Zhao, J. Qu, K. Li, Y. Liu, L. Wang, and L. Bu, "A novel underactuated exoskeleton rehabilitation glove for hand flexion and extension training," *Biomimetic Intelligence and Robotics*, vol. 5, no. 4, p. 100248, 2025, https://doi.org/10.1016/j.birob.2025.100248.

[12] K. Rsetam, Z. Cao and Z. Man, "Design of Robust Terminal Sliding Mode Control for Underactuated Flexible Joint Robot," in *IEEE Transactions on Systems, Man, and Cybernetics: Systems*, vol. 52, no. 7, pp. 4272-4285, 2022, https://doi.org/10.1109/TSMC.2021.3096835.

[13] W. F. Faris, M. Rabie, A. O. Moaaz, N. M. Ghazaly, and M. M. Makrahy, "Two-flexible-link manipulator vibration reduction through fuzzy-based position," *International Journal of Robotics & Control Systems*, vol. 5, no. 1, p. 479, 2025, https://doi.org/10.31763/ijrcs.v5i1.1669.

[14] W. Li and X. Zhang, "Data-driven model predictive control for underactuated usv path tracking with unknown dynamics," *Ocean Engineering*, vol. 333, p. 121457, 2025, https://doi.org/10.1016/j.oceaneng.2025.121457.

[15] J. Bettega and D. Richiedei, "Trajectory tracking in an underactuated, non-minimum phase two-link multibody system through model predictive control with embedded reference dynamics," *Mechanism and machine theory*, vol. 180, p. 105165, 2023, https://doi.org/10.1016/j.mechmachtheory.2022.105165.

[16] K. Saoudi, E. K. Bdirina and K. Guesmi, "Model Predictive Sliding Mode Control for a Class of Affine Nonlinear Systems," *2022 International Conference of Advanced Technology in Electronic and Electrical Engineering (ICATEEE)*, pp. 1-6, 2022, http://doi.org/10.1109/ICATEEE57445.2022.10093734.

[17] M. L. Castaño and X. Tan, "Backstepping-Based Tracking Control of Underactuated Aquatic Robots," in *IEEE Transactions on Control Systems Technology*, vol. 31, no. 3, pp. 1179-1195, 2023, https://doi.org/10.1109/TCST.2022.3215585.

[18] Z. Madni, K. Guesmi, and A. Benalia, "Backstepping global and structural stabilization of direct current/direct current boost converter," *International Journal of Circuit Theory and Applications*, vol. 50, no. 5, pp. 1604–1619, 2022, https://doi.org/10.1002/cta.3237.

[19] Y. Yang, X. Ye, B. Wen, J. Huang, and X. Su, "Adaptive control design for uncertain underactuated cranes with nonsmooth input nonlinearities," *IEEE Transactions on Systems, Man, and Cybernetics: Systems*, vol. 53, no. 2, pp. 1074–1083, 2022, https://doi.org/10.1109/TSMC.2022.3192754.

[20] A. Y. Damani, Z. A. Benselama, and R. Hedjar, "Formation control of nonholonomic wheeled mobile robots using adaptive distributed fractional order fast terminal sliding mode control," *Archive of Mechanical Engineering*, vol. 70, no. 4, pp. 567–587, 2023, https://doi.org/10.24425/ame.2023.148700.

[21] A. Rebai, K. Guesmi, and M. Bougrine, "Design of an adaptive fuzzy backstepping synergetic control scheme," in *Proceedings of the 4th International Conference on Electrical Engineering and Control Applications: ICEECA*, vol. 682, p. 263, 2020, https://doi.org/10.1007/978-981-15-6403-1_18.

[22] B. Lu and Y. Fang, "Gain-adapting coupling control for a class of underactuated mechanical systems," *Automatica*, vol. 125, p. 109461, 2021, https://doi.org/10.1016/j.automatica.2020.109461.

[23] N. Jiang, D. Guo, S. Zhang, D. Zhang, and J. Xu, "Cascade control of underactuated manipulator based on reinforcement learning framework," *Proceedings of the Institution of Mechanical Engineers, Part I: Journal of Systems and Control Engineering*, vol. 237, no. 2, pp. 231–243, 2023, https://doi.org/10.1177/09596518221125533.

[24] J. -X. Zhang, T. Yang and T. Chai, "Neural Network Control of Underactuated Surface Vehicles With Prescribed Trajectory Tracking Performance," in *IEEE Transactions on Neural Networks and Learning Systems*, vol. 35, no. 6, pp. 8026-8039, 2024, https://doi.org/10.1109/TNNLS.2022.3223666.

[25] L. Wang, W. Jiang, L. Zhao, and Z. Jiao, "Neural network based position control of an underactuated flapping wing aircraft considering the aerodynamic damping," *Nonlinear Dynamics*, vol. 112, no. 15, pp. 13249–13267, 2024, https://doi.org/10.1007/s11071-024-09735-0.

[26] D. -B. Pham, T. -v. -A. Nguyen and N. -T. Bui, "Composite Fuzzy-Based Control Strategy for Uncertain Underactuated System," in *IEEE Access*, vol. 12, pp. 155564-155577, 2024, https://doi.org/10.1109/ACCESS.2024.3485243.

[27] H. Gong, M. J. Er, and Y. Liu, "Fuzzy adaptive optimal fault-tolerant trajectory tracking control for underactuated auvs with input saturation," *Ocean Engineering*, vol. 311, p. 118940, 2024, https://doi.org/10.1016/j.oceaneng.2024.118940.

[28] X. -P. Nguyen, X. -K. Dang, V. -D. Do, J. M. Corchado and H. -N. Truong, "Robust Adaptive Fuzzy-Free Fault-Tolerant Path Planning Control for a Semi-Submersible Platform Dynamic Positioning System With Actuator Constraints," in *IEEE Transactions on Intelligent Transportation Systems*, vol. 24, no. 11, pp. 12701-12715, 2023, https://doi.org/10.1109/TITS.2023.3297252.

[29] K. Guesmi, A. Hamzaoui and J. Zaytoon, "Fuzzy controller synthesis for a DC-DC converter," *Proceedings of the 48h IEEE Conference on Decision and Control (CDC) held jointly with 2009 28th Chinese Control Conference*, pp. 3106-3111, 2009, https://doi.org/10.1109/CDC.2009.5400184.

[30] M. Mattioni and P. Borja, "Digital passivity-based control of underactuated mechanical systems," *Automatica*, vol. 173, p. 112096, 2025, https://doi.org/10.1016/j.automatica.2024.112096.

[31] D. Gutiérrez-Oribio, I. Stefanou, and F. Plestan, "Passivity-based control of underactuated mechanical systems with coulomb friction: Application to earthquake prevention," *Automatica*, vol. 165, p. 111661, 2024, https://doi.org/10.1016/j.automatica.2024.111661.

[32] D. N. Cardoso, S. Esteban, and G. V. Raffo, "A robust optimal control approach in the weighted sobolev space for underactuated mechanical systems," *Automatica*, vol. 125, p. 109474, 2021, https://doi.org/10.1016/j.automatica.2020.109474.

[33] G. Rigatos, "Nonlinear optimal control for the underactuated double-pendulum overhead crane," *Journal of Vibration Engineering & Technologies*, vol. 12, no. 2, pp. 1203–1223, 2024, https://doi.org/10.1007/s42417-023-00902-y.

[34] D. Huixuan, W. Sun, and Z. Chenglong, "Adaptive fuzzy sliding mode control for underactuated systems with time-varying sensor faults," *Journal of the Chinese Institute of Engineers*, vol. 47, no. 3, pp. 351–358, 2024, https://doi.org/10.1080/02533839.2024.2308251.

[35] H. Zou and M. Wang, "Enhanced sliding-mode control for tracking control of uncertain fractional-order nonlinear systems based on fuzzy logic systems," *Applied Sciences*, vol. 15, no. 9, p. 4686, 2025, https://doi.org/10.3390/app15094686.

[36] O. Mofid and S. Mobayen, "Adaptive sliding mode control for finite-time stability of quad-rotor uavs with parametric uncertainties," *ISA transactions*, vol. 72, pp. 1–14, 2018, https://doi.org/10.1016/j.isatra.2017.11.010.

[37] O. Mofid, S. Mobayen, C. Zhang, and B. Esakki, "Desired tracking of delayed quadrotor uav under model uncertainty and wind disturbance using adaptive super-twisting terminal sliding mode control," *ISA transactions*, vol. 123, pp. 455–471, 2022, https://doi.org/10.1016/j.isatra.2021.06.002.

[38] A. Mousavi and A. H. Markazi, "Adaptive fuzzy sliding-mode control of under-actuated systems with unknown input gain function," *Proceedings of the Institution of Mechanical Engineers, Part C: Journal of Mechanical Engineering Science*, vol. 238, no. 12, pp. 5455–5468, 2024, https://doi.org/10.1177/09544062231207456.

[39] A. Mohammadzadeh, H. Taghavifar, C. Zhang, K. A. Alattas, J. Liu, and M. T. Vu, "A non-linear fractional-order type-3 fuzzy control for enhanced path-tracking performance of autonomous cars," *IET Control Theory & Applications*, vol. 18, no. 1, pp. 40–54, 2024, https://doi.org/10.1049/cth2.12538.

[40] M. A. Balootaki, H. Rahmani, H. Moeinkhah, and A. Mohammadzadeh, "Non-singleton fuzzy control for multi-synchronization of chaotic systems," *Applied Soft Computing*, vol. 99, p. 106924, 2021, https://doi.org/10.1016/j.asoc.2020.106924.

[41] A. S. Alkabaa, O. Taylan, M. Balubaid, C. Zhang, and A. Mohammadzadeh, "A practical type-3 fuzzy control for mobile robots: predictive and boltzmann-based learning," *Complex & Intelligent Systems*, vol. 9, no. 6, pp. 6509–6522, 2023, https://doi.org/10.1007/s40747-023-01086-4.

[42] S. Xu, C. Zhang, and A. Mohammadzadeh, "Type-3 fuzzy control of robotic manipulators," *Symmetry*, vol. 15, no. 2, p. 483, 2023, https://doi.org/10.3390/sym15020483.

[43] A. Taghieh, A. Mohammadzadeh, C. Zhang, S. Rathinasamy, and S. Bekiros, "A novel adaptive interval type-3 neuro-fuzzy robust controller for nonlinear complex dynamical systems with inherent uncertainties," *Nonlinear Dynamics*, vol. 111, no. 1, pp. 411–425, 2023, https://doi.org/10.1007/s11071-022-07867-9.

[44] H. M. Cuong, N. T. Lam, H. Q. Dong, P. Van Trieu, N. H. Tuan and L. A. Tuan, "Fractional-order terminal sliding mode control for a class of underactuated nonlinear systems," *2020 IEEE 18th International Conference on Industrial Informatics (INDIN)*, pp. 703-706, 2020, https://doi.org/10.1109/INDIN45582.2020.9442124.

[45] O. Mofid and S. Mobayen, "Robust fractional-order sliding mode tracker for quad-rotor uavs: event-triggered adaptive backstepping approach under disturbance and uncertainty," *Aerospace Science and Technology*, vol. 146, p. 108916, 2024, https://doi.org/10.1016/j.ast.2024.108916.

[46] F. U. Rehman, N. Mehmood, S. U. Din, M. R. Mufti and H. Afzal, "Adaptive Sliding Mode Based Stabilization Control for the Class of Underactuated Mechanical Systems," in *IEEE Access*, vol. 9, pp. 26607-26615, 2021, https://doi.org/10.1109/ACCESS.2021.3057667.

[47] M. Idrees, S. Ullah, and S. Muhammad, "Sliding mode control design for stabilization of underactuated mechanical systems," *Advances in Mechanical Engineering*, vol. 11, no. 5, p. 1687814019842712, 2019, https://doi.org/10.1177/1687814019842712.

[48] R. G. Roy and N. Olgac, "Robust nonlinear control via moving sliding surfaces-n-th order case," in *Proceedings of the 36th IEEE Conference on Decision and Control*, vol. 2, pp. 943–948, 1997, https://doi.org/10.1109/CDC.1997.657564.

[49] A. Dumlu, "Design of a fractional-order adaptive integral sliding mode controller for the trajectory tracking control of robot manipulators," *Proceedings of the Institution of Mechanical Engineers, Part I: Journal of Systems and Control Engineering*, vol. 232, no. 9, pp. 1212–1229, 2018, https://doi.org/10.1177/0959651818778218.

[50] W. AlAlaween, A. H. AlAlawin, B. M. Gharaibeh, M. Mahfouf, A. Alsoussi, S. O. AbuHamour, and A. E. AbuKaraky, "A type-1 fuzzy fusion model based on the dempster-shafer theory for the simulation of 3d fused deposition," *Journal of Intelligent & Fuzzy Systems*, p. 18758967251334236, 2025, https://doi.org/10.1177/18758967251334236.

[51] Y. Su, F. Teng, T. Li, H. Liang and C. L. Philip Chen, "Fuzzy-Based Optimal Control for an Underactuated Surface Vessel With User-Specified Performance," in *IEEE Transactions on Intelligent Transportation Systems*, vol. 26, no. 5, pp. 7036-7050, 2025, https://doi.org/10.1109/TITS.2025.3526758.

[52] R. Chotikunnan, P. Chotikunnan, P. Imura, Y. Pititheeraphab, and N. Thongpance, "The utilization of fuzzy logic controllers in steering control systems for electric ambulance golf carts," *International Journal of Robotics and Control Systems*, vol. 4, no. 1, pp. 427–444, 2024, https://doi.org/10.31763/ijrcs.v4i1.1333.

[53] M. Aydin, G. Camliyurt, M. Gul, S. I. Sezer, E. Celik, and E. Akyuz, "An interval type-2 fuzzy marcos modelling to assess performance effectiveness of survival craft on cargo ship," *Ocean Engineering*, vol. 326, p. 120899, 2025, https://doi.org/10.1016/j.oceaneng.2025.120899.

[54] C. Sun, K. Mei, L. Ma, S. Ding, Y. Li, and C. Ding, "Adaptive type-2 fuzzy hosm control design with asymmetric output constraints," *Nonlinear Dynamics*, vol. 113, pp. 27895–27911, 2025, https://doi.org/10.1007/s11071-025-11586-2.

[55] S. A. Moafi and F. Najafi, "Interval type-2 fuzzy-logic-based impedance control of a hip joint rehabilitation robot driven by a high-order sliding-mode-controlled series elastic actuator," *International Journal of Intelligent Robotics and Applications*, vol. 9, no. 1, pp. 21–46, 2025, https://doi.org/10.1007/s41315-025-00426-6.

[56] A. Mohammadzadeh, M. H. Sabzalian, and W. Zhang, "An interval type-3 fuzzy system and a new online fractional-order learning algorithm: theory and practice," *IEEE Transactions on Fuzzy Systems*, vol. 28, no. 9, pp. 1940–1950, 2019, https://doi.org/10.1109/TFUZZ.2019.2928509.

[57] A. Mohammadzadeh, M. T. Vu, H. Taghavifar, K. A. Alattas, R. Sakthivel, and C. Zhang, "A type-3 fuzzy logic system with uncertainty bound type-reduction and optimized secondary memberships and level of alpha-cuts," *International Journal of Fuzzy Systems*, pp. 1–12, 2025, https://doi.org/10.1007/s40815-025-02082-1.

[58] A. Mohammadzadeh, K. A. Alattas, W. -F. Xie, H. Taghavifar, C. Zhang and R. Sakthivel, "T3-ANFIS: Type-3 Adaptive Neuro-Fuzzy Inference System With a Noniterative Learning Algorithm," in *IEEE Transactions on Cybernetics*, vol. 55, no. 11, pp. 5387-5400, 2025, https://doi.org/10.1109/TCYB.2025.3591897.

[59] S. L. Brunton and J. N. Kutz, *Data-driven science and engineering: Machine learning, dynamical systems, and control*, Cambridge University Press, 2019, https://doi.org/10.1017/9781108380690.

[60] H.-S. Kang, Y. Lee, C.-H. Hyun, H. Lee, and M. Park, "Design of sliding-mode control based on fuzzy disturbance observer for minimization of switching gain and chattering," *Soft Computing*, vol. 19, no. 4, pp. 851–858, 2015, https://doi.org/10.1007/s00500-014-1412-8.